

# A study of OH and H<sub>2</sub>O masers in the circumstellar envelopes around Miras

K. Murakawa<sup>1,2</sup>, J. A. Yates<sup>3</sup>, A. M. S. Richards<sup>4</sup>, R. J. Cohen<sup>4</sup>, and H. J. van Langevelde<sup>5</sup>

<sup>1</sup> Subaru telescope, 650 North A'ohoku Place, Hilo, HI 96720, USA Department of physical science, University of Hertfordshire, College Lane, Hatfield, Herts, AL10 9AB, United Kingdom

<sup>2</sup> Department of Physics and Astronomy, University College London, Gower Street, London WC1E 6BT, United Kingdom

<sup>3</sup> Nuffield Radio Astronomy Laboratories, University of Manchester, Jodrell Bank, Macclesfield, Cheshire SK11 9DL, England, United Kingdom

<sup>4</sup> Joint Institute for VLBI in Europe, Radiosterrenwacht Dwingeloo, Postbus 2, 7990 AA Dwingeloo, the Netherlands

**Abstract.** We have obtained OH and H<sub>2</sub>O maser emission map of U Ori using the EVN and MERLIN. We achieve a spatial resolution of about 10 mas for both maser emission lines. Our maps show that H<sub>2</sub>O masers are found close to the star, in a well-filled shell with an equatorial density enhancement around U Ori. The OH main line masers appear to spread biconically out of the water maser shell along the polar axis. It is possible that greater star light penetration in these directions favours the OH maser population inversion.

## 1. Introduction

When stars with intermediate mass ( $<8M_{\odot}$ ) reaches at asymptotic giant branch (AGB) phase, their mass loss event becomes active and up to 90% of their initial mass are lost. Investigation of mass losing is very important to study the evolution of late type star.

A traditional "onion shell" model for O-rich AGB or red supergiant (RSG) contains SiO, H<sub>2</sub>O and OH maser regions at increasing distances from the star (e.g. Goldreich & Scoville 1976). Combining these emission maps with velocity structures, the 3D structure of stellar wind can be investigate.

U Orionis is one of the brightest long-period variables belonging to the Mira Ceti type. Kholopov et al. (1985) shows its period of 368 days and its visual brightness and spectral types varies 4.8-13.0 mag and from M6e and M9.5e, respectively. U Ori is known to be a source of maser radio emission of OH (Wilson & Barrett 1970), H<sub>2</sub>O (Wilson et al. 1972) and SiO (Kaifu et al. 1975). The mass loss rate and the stellar velocity have been estimated  $2.9 \times 10^{-7} M_{\odot} \text{yr}^{-1}$  from the thermal CO line and  $-38.1 \pm 1.3 \text{ km s}^{-1}$ , respectively. A recent distance estimate for U Ori, using the P-M<sub>k</sub> dependence and the Hipparcos data, is  $\sim 300$  pc (Knapp et al. 1998).

We have obtained OH and H<sub>2</sub>O maser emission maps of U Ori in the same year of 1999. The important things are (1) high resolution imaging from small to large scale, (2) measuring changes of structure in time, and (3) use the chemical properties of the wind to place limits on the density structure and investigate latitude dependent mass losing. In this paper, we will compare OH and H<sub>2</sub>O maser emission line maps and discuss the mass loss event of U Ori.

## 2. Observation and results

We have used European VLBI/global network (EVN) and Multi-Element Radio Linked Networks (MERLIN) to observe OH mainlines masers (1665 and 1667MHz) and H<sub>2</sub>O maser (22 GHz) of U Ori. Seven antennas with the maximum baseline of 2279 km were used for EVN. The angular resolution and velocity resolution are about 30 mas and  $0.2 \text{ km s}^{-1}$ , respectively. Five antennas with the maximum baseline of 217 km were used for MERLIN. The angular resolution and the velocity resolution are about 10 mas and  $0.1 \text{ km s}^{-1}$ . In any experiment, a quasar 3C 84 was observed for calibration of the flux.

We reduced the data as described in Richards et al. 1999 for MERLIN data and followed van Langevelde for EVN data using AIPS. The data weighted for the best combination of resolution and sensitivity, mapped in total intensity and CLEANed using the AIPS task IMAGR. We fitted 2-D Gaussian components to each patch of emission in each channel in each data cube in order to measure the peak flux density, the position relative to the reference feature used for self-calibration, the total area of the component and the total flux density. The relative position uncertainty is typically 1 mas. The fitted components were grouped into features if three or more components with  $\text{SN} > 3\sigma$  occurred in adjacent channels with positions overlapping to within the position error or component size. Non-matched components were discarded, as were any others which coincided with beam side lobes.

Fig1. shows a velocity distribution of H<sub>2</sub>O maser emission line. There is a single peak located at  $-38.2 \text{ km s}^{-1}$  in our experiment and its velocity range varies from  $-37$  to  $-38.7 \text{ km s}^{-1}$ . The velocity distribution of OH maser has multi-peak structure and varies from  $-35$  to  $-40 \text{ km s}^{-1}$ .

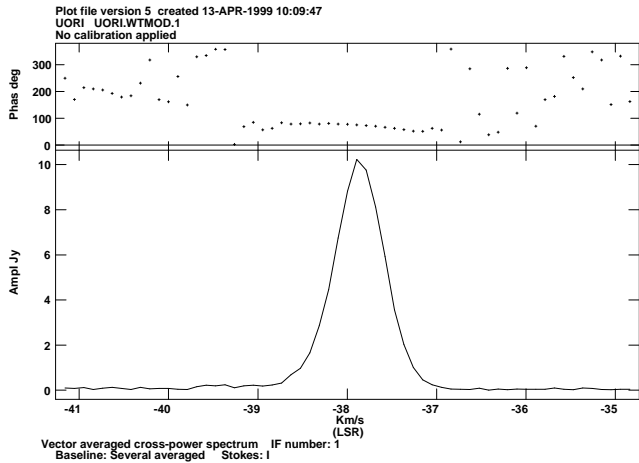


**Fig. 1.** The velocity distribution of H<sub>2</sub>O maser emission line of U Ori. The peak flux is located at  $-38.2 \text{ kms}^{-1}$ .

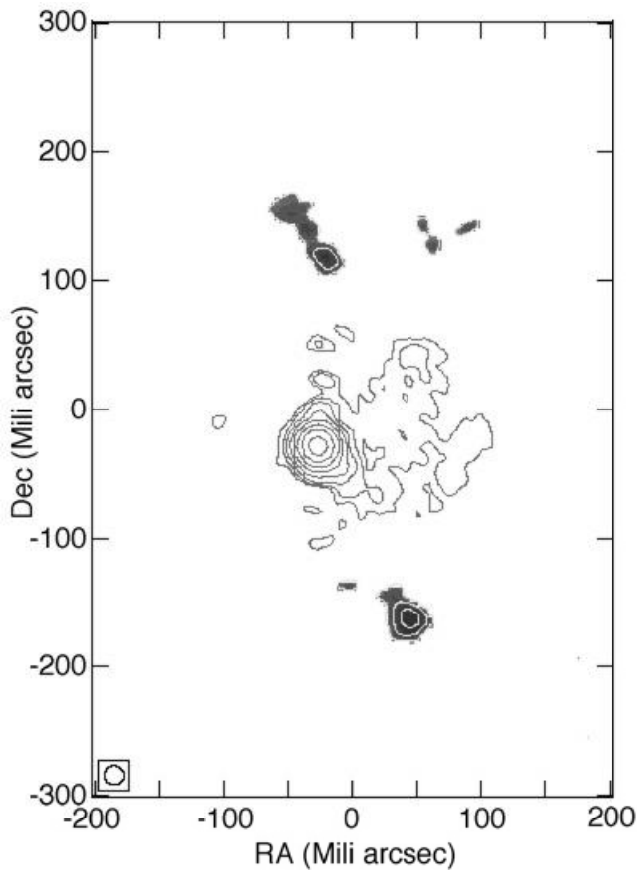


**Fig. 2.** A composite image of OH and H<sub>2</sub>O maser emission maps. The central contour map is for the H<sub>2</sub>O maser and the North and the South gray scale spots with contour maps are for the OH maser.

OH maser spots are split into the North and the South parts with separation of 250 mas.

### 3. Discussions

Fig.2 shows a composite image of OH maser emission line map and H<sub>2</sub>O maser emission line map. The central con-

tour is of the H<sub>2</sub>O maser and OH maser spots are splitting into the North and the South. For H<sub>2</sub>O maser emission line, while the strong peak is located at  $-38.2 \text{ kms}^{-1}$ , weak peaks at the West are located at  $-37.9 \text{ kms}^{-1}$  and  $-40.8$  to  $-42.6 \text{ kms}^{-1}$ . There is a possibility that the discrepancy of the both peaks is due to rotation of the circumstellar envelope with the NS axis. If this is real, it can be interpreted that H<sub>2</sub>O maser spots localise in the EW lane due to the equatorial enhancement. Furthermore, existence of OH maser spots at the North and the South could be that star light can escape toward the North and the South and can play a role in favours the OH maser population inversion while it could be absorbed by thick H<sub>2</sub>O maser cloud in WE direction.

However, we have to pay attention before making conclusions about the scenario above. Because the H<sub>2</sub>O maser spots obtained in 1994 (Bains et al. in preparation) don't show like Fig. 2. H<sub>2</sub>O maser emission line map in 1994 shows that the most dominant peak is located at the SW and a few small spots scatters at NE while the velocity distribution shows similar structure to that in 1999. No proof of rotation can be seen in 1994 data. While it is confirmed that OH maser spots obtained by Chapman et al. 1991 in 1987 are split into the North and the South and its feature has been comparably stable for more 10 years, H<sub>2</sub>O maser spots changes in their feature during 5 years as described above (also see Rudnitskij et al. 2000). To conclude above scenario, more observations are required. Monitoring both H<sub>2</sub>O maser emission line and OH maser emission lines simultaneously are important way to investigate the relationship between these maser feature.

*Acknowledgements.* K.M. acknowledges support as a PPARC funded PDRA at the University of Hertfordshire. H.J.v.L. acknowledges partial support from the EC ICN RadioNET (Contract No. HPRI-CT-1999-40003).

### References

- Bains, I., Cohen, R. J., Louridas, A., Richards, A. M. S., Rosa-Gonzales, D., & Yates, J. A., MNRAS, in preparation
- Chapman, J. M., Cohen, R. J., & Saikia, D. J., 1991, MNRAS, 249, 227
- Goldreich, P., & Scoville, N., 1976, ApJ, 205, 144
- Kaifu, N., Buhl, D., & Snyder, L. E., 1975, ApJ, 249, 118
- Kholopov P. N., Samus' N. N., Frolov, M. S. et al., General Catalogue of Variable Stars, Vol. II, Nauka, Moscow, 1985, p. 278
- Knapp, G. R., Young, K., Lee, E., & Jorissen, A., 1998, ApJS, 117, 209
- Richards, A. M. S., Yates, A. J., & Cohen, R. J., 1999, MNRAS, 306, 954
- Rudnitskij, G. M., Lekht, E. E., Mendoza-Torres, J. E., Pashchenko, M. I., & Berulis, I. I., 2000, A&ASS, 146, 385
- Wilson, W. J., & Barrett, A. H., 1970, Kitt Peak Nat. Observ. Contr. 554, 77
- Wilson, W. J., Schwartz, P. R., Neugebauer, G., Harvey, P. M., & Becklin, E. E., 1972, ApJ, 177, 523